KAWASAKI STEEL TECHNICAL REPORT
No.1 (September 1980)

Recent Progress of OBM/Q-BOP Steelmaking at Kawasaki Steel Corporation

Kyoji Nakanishi, Tsutomu Nozaki, Ryoji Uchimura, Toyohiko Ohta, Makoto Saigusa, Jun Nagai, Fumio Sudo

Synopsis :
Kawasaki has succeeded in prolongation of the bottom life of the Q-BOP:2063 heats at the maximum and 1500 heats on an average. A newly developed method, "Panel AE Spalling Test", has shown the magnesia-carbon brick to be most preferable for bottom refractories. The OG gas recovered from the Q-BOP contains the latent heat exceeding 2700kcal/Nm3. Kawasaki has completed the dynamic control system called "SMART" which has contributed to a marked improvement of hit rate for both carbon and temperature at turn-down with the highest record of 98.8%. For a given temperature and slag composition, the steel made in the Q-BOP contains more manganese, less oxygen and less sulfur than that of the LD. The lowest carbon levels are 0.01% while blowing oxygen and 0.006% by rinsing with inert gas. Both are quite lower than those of the LD. To comprehensively interpret all the oxidizing furnaces such as the Q-BOP, the LD and the AOD, a new parameter ISCO has been proposed. ISCO stands for Index for Selective Carbon Oxidation, which consists of a chemical and a kinetic terms. The validity of ISCO has been shown in connection with the dephosphorization reaction and the chromium oxidation.

The body can be viewed from the next page.

Recent Progress of OBM/Q-BOP Steelmaking at Kawasaki Steel Corporation*

Kyoji NAKANISHI** Tsutomu NOZAKI** Ryoji UCHIMURA**
Toyohiko OHTA** Makoto SAIGUSA*** Jun NAGAI***
Fumio SUDO***

Kawasaki has succeeded in prolongation of the bottom life of the Q-BOP: 2 063 heats at the maximum and 1500 heats on an average. A newly developed method, "Panel AE Spalling Test", has shown the magnesia-carbon brick to be most preferable for bottom refractories. The OG gas recovered from the Q-BOP contains the latent heat exceeding 2 700 kcal/Nm³. Kawasaki has completed the dynamic control system called "SMART" which has contributed to a marked improvement of hit rate for both carbon and temperature at turn-down with the highest record of 98.8%.

For a given temperature and slag composition, the steel made in the Q-BOP contains more manganese, less oxygen and less sulfur than that of the LD. The lowest carbon levels are 0.01% while blowing oxygen and 0.006% by rinsing with inert gas. Both are quite lower than those of the LD. To comprehensively interpret all the oxidizing furnaces such as the Q-BOP, the LD and the AOD, a new parameter ISCO has been proposed. ISCO stands for Index for Selective Carbon Oxidation, which consists of a chemical and a kinetic terms. The validity of ISCO has been shown in connection with the dephosphorization reaction and the chromium oxidation.

1 Introduction

The OBM/Q-BOP technology has taken a great stride forward in the last decade toward an economical mass-production process which even surpasses the conventional LD. Since February 1977, two Q-BOP furnaces of 230 t have been smoothly in operation at Chiba Works of Kawasaki Steel Corporation. Among many records so far established at Kawasaki, an outstanding is of 2 063 heats for the bottom life attained on April 4th, 1980.

In the Q-BOP oxygen gas is injected together with powdered burnt lime from tuyeres at the bottom of the bath. Metallurgically this brings unique features of the Q-BOP in comparison with the LD.

This paper describes both the technological development of the Q-BOP and its metallurgical and chemical aspects recently obtained at Kawasaki.[1-5, 8-11, 14]

* Received on May 6, 1980
** Research Laboratories
*** Chiba Works

2 Brief Description of Q-BOP Shop at Chiba

Two units of 230 t OBM/Q-BOP vessels are installed at No. 3 Steelmaking Shop of Chiba Works. The unlined vessel has an inner volume of 487.4 m³. The bottom has 18 tuyeres, from which oxygen gas is fed at the normal flow rate of 700 Nm³/min.

In **Photo. 1**, the hot metal is being charged into one of the Q-BOP furnaces. Normally one vessel out of two is operated. At present the production rate is about 250 thousand ton of steel per month. The tuyere consists of two concentric pipes, where oxygen and powdered burnt lime are fed through the inner pipe and the propane is fed through the annular slit to protect the tuyere.

3 Technological Development

3.1 Prolongation of Bottom and Barrel Lives[1-2, 14]

Several years ago it was thought that a rather short bottom life was a serious drawback to the future expansion of the OBM/Q-BOP process. Especially in the vicinity of tuyeres the bottom refractories undergo

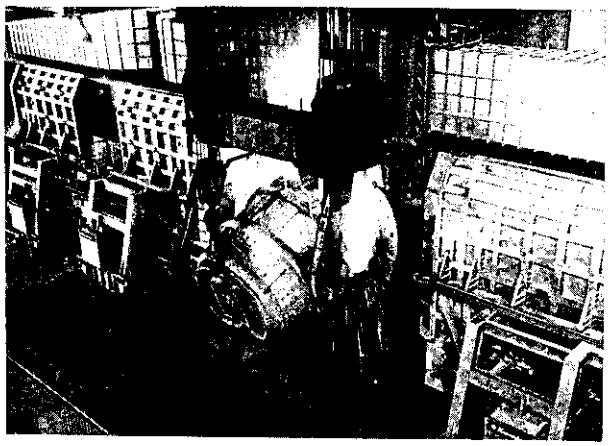

Photo. 1 Hot metal being charged into one of Kawasaki's new 230 t Q-BOP furnaces

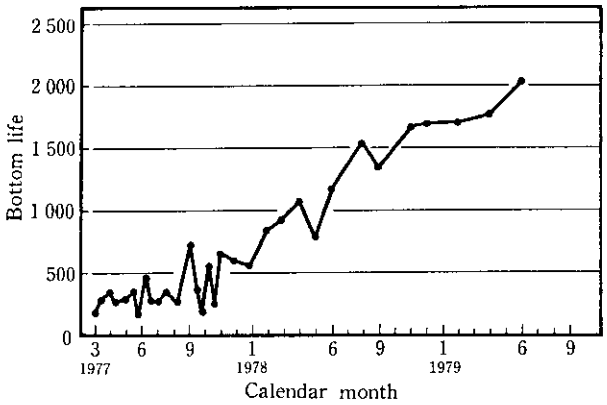

Fig. 1 Trend of bottom performance of Q-BOP at Chiba Works

a great change in the distribution of temperature; thus they were reported to be seriously worn out. However, as shown in **Fig. 1**, Kawasaki has proved that the bottom life is drastically prolonged by proper refractories together with the improved brickwork and slag coating technique.

The barrel life has also improved markedly from the start. The barrel and the bottom lives have reached at their highest levels more than 3 500 and 2 000 heats, respectively. On an average, the barrel life is 3 000 heats while the bottom life is 1 500 heats. Therefore, the Q-BOP has economically come to be quite competitive with the LD process in terms of refractory consumption.

Among many improvements added in the process of the development of refractories, brickwork and operations, the most conspicuous one is the use of newly developed magnesia-carbon refractories which, because of their remarkably high thermal conductivities exhibit highly resistance against thermal spalling. The magnesia-carbon refractories are particularly used around tuyeres where temperature varies widely and rapidly. Of all the properties of refractory required, the spalling resistance is most important, and yet a lack of reliable testing methods which enable accurately to predict performabilities of refractories under actual operating conditions, makes the available data of little value. At Research Laboratories of Kawasaki, a new testing method, "Panel-AE Spalling Test" has successfully been developed.[3]

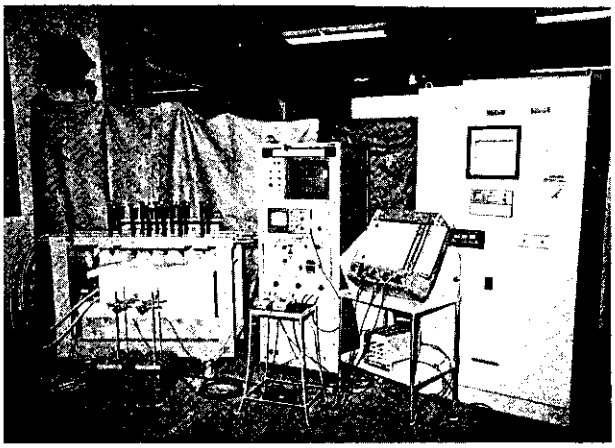

Photo. 2 Apparatus for "panel AE spalling test"

The feature of this testing method lies in detecting the initiation and propagation of cracks generated in the bulk of refractories by means of the acoustic emission(AE) technique. This ensures a much higher sensitivity and accuracy than those of conventional testing methods which rely heavily on visual inspection of cracks. **Photo. 2** shows the testing apparatus which consists of an electric furnace, its temperature control unit, a cooling device which is used to give a certain temperature gradient or a certain cooling rate, the AE measuring system and a steel frame in which a refractory panel is constructed. By using the panel AE spalling test, the magnesia-carbon has been found to be the most preferable for the bottom refractories of the Q-BOP.

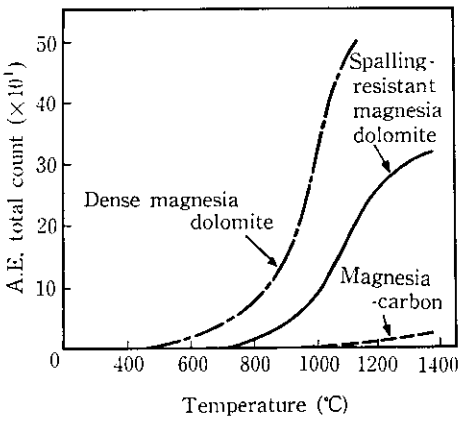

Fig. 2 Typical results of panel-AE spalling test

As a typical example, the panel spalling tests were made for three different types of refractories at the heating rate of 20 °C/min. **Fig. 2** shows the results where total counts of AE are plotted against temperatures measured at the hot faces of the specimens; obviously the magnesia-carbon brick is extremely superior to the others. As mentioned above, this was also practically verified.

At the practical Q-BOP operation the addition of dolomitic lime is effective to prevent the dissolution of magnesia out of refractories into the slag. In comparison with the LD, the consumption of dolomitic lime is cut down, probably due to the lower concentration of iron oxide in the slag and non-existence of superheat in the slag.[1]

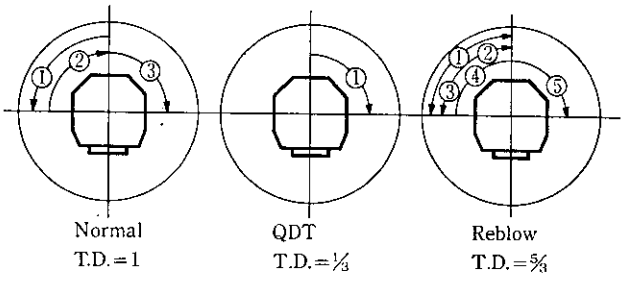

Fig. 3 Illustration of turn-down index

The bottom wearing rate is also affected by the tilting frequency of the furnace[4], which is tentatively designated by TD (Turn-Down Index) illustrated in **Fig. 3** and given by Eq. **(1)**,

$$TD = \frac{n_N + n_Q/3 + 5n_R/3}{n_N + n_Q + n_R} \quad \cdots\cdots\cdots\cdots (1)$$

where n_N is the number of heats blown normally through one campaign, n_Q is the number of heats blown by QDT which stands for Quick and Direct Tapping, the detailed description of which is given later, and n_R is the number of heats reblown through one campaign. **Fig. 4** shows the relationship of the bottom wearing rate and the value of TD; obviously the bottom wearing rate increases with an increase of TD value.

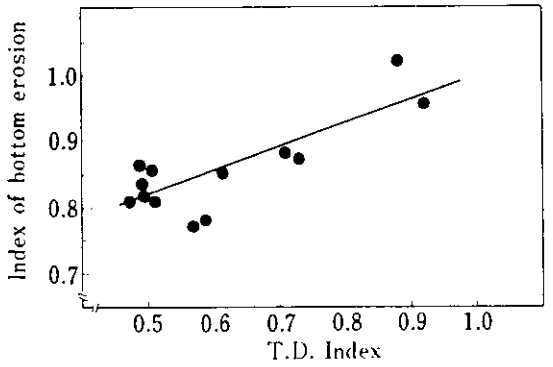

Fig. 4 Bottom wearing rate vs. turn-down index relationship

3.2 Recovery of Off-gas

Kawasaki's Q-BOP's are firstly in the world installed with the OG recovery system. Ever since they started, the amount of the combustible gas recovered has increased and marked the highest record of 251 $\times 10^3$ kcal/t in Sept. 1978. The secondary combustion of the gas with the air is strongly affected by the opening between the converter mouth and the hood skirt; therefore this opening should be kept at minimum to avoid the secondary combustion. Fortunately, with the absence of slopping which often takes place in the LD process, the opening is kept 30 mm at the normal operation of the Q-BOP. In addition, a higher efficiency of decarburization is the another favorable characteristic of the Q-BOP to procure a higher gas recovery than that of the LD process. As a result, being shown in **Table 1**, the OG gas of the Q-BOP contains much more CO and H_2 than those of the LD; hence the heat of combustion of the OG gas, i.e., the latent heat exceeds 2 700 kcal/Nm^3. About 86.4% of total energy is recovered as the OG gas and the steam, 5% of which comes from the propane gas used for the protection of tuyeres.

Table 1 Chemical composition of off-gas from Q-BOP and LD

	CO	CO_2	H_2	N_2
Q-BOP	86.3%	2.8%	5.6%	5.3%
LD (Chiba)	64.5	18.4	0.7	16.4

3.3 Dynamic Control System and QDT

3.3.1 Dynamic control system, "SMART"

Kawasaki's Q-BOP is installed with a sensor lance which provides us with one point check for chemical composition and temperature of the bath in the course of blowing.

It was in April 1978 that Kawasaki completed the system called SMART (System for Measuring and Attaining Refining Target) which covered the unique features of metallurgical reactions occurring in the Q-BOP furnace.

SMART has the following three important items: mathematical equations of the static model, mathematical equations of the dynamic model, and the sensor lance and auxiliary equipment made by Kawa-

saki, which provided us with fully automated manipulations of setting a test probe, measuring, withdrawing a sample for chemical analyses, and so forth.

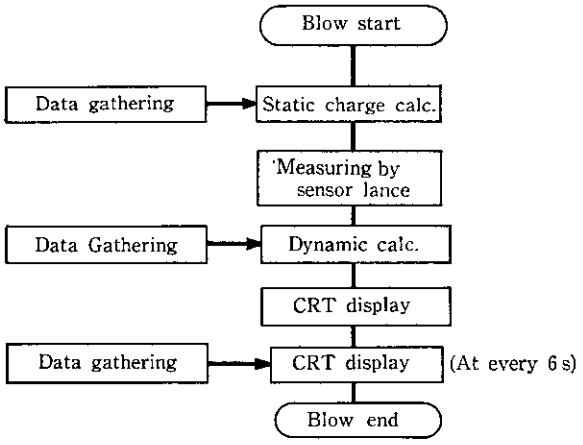

Fig. 5 Block diagram of SMART

Fig. 5 shows the block diagram of SMART. By using mathematical equations of the static model, a preliminary calculation is made in advance for total amounts of oxygen and iron ore. Carbon content and temperature of molten steel are measured by the sensor lance at a later stage of blowing. The resultant data are automatically read by a process computer, which, on the basis of the dynamic control model, calculates amounts of oxygen and iron ore needed to hit aiming carbon content and temperature. At the same time the computer displays predicted carbon content and temperature on the CRT at every 60 Nm^3 oxygen blown, as shown in **Fig. 6**. The sensor lance is put in practical use with nearly no exception. Since one cycle requires only 110 seconds, multiple measurements are possible within a normal blowing duration. In common practice, however, only one measurement suffices to attain aiming carbon content and temperature at the end of blow. The mathematical equations of the static model are substantially based on the heat balance and the mass balance; hence nothing particular to be emphasized. On the other hand, there is one thing to be stressed on the mathematical equations of the dynamic model; namely, the accumulated amount of oxygen in the slag is quantitatively taken into account so as to achieve a highly accurate prediction of carbon content at the end of blow.

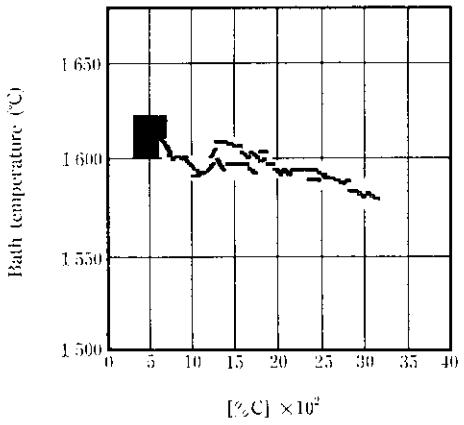

Fig. 6 Typical example of CRT display by SMART

Table 2 Advantages of Q-BOP over LD for end-point control

	Q-BOP	BOP
Blowing	Stable	Unstable
Reproducibility	Superior	Inferior
Easiness of basicity calculation	B.(act.)=B.(cal.)	B.(act.)<B.(cal.)
Fe recovery from ore	100 %	<100 %
(T.Fe) in slag	Stable	Unstable
$-\frac{dC}{dO_2}$	Stable	Unstable

The several advantages of the Q-BOP relevant to end-point control are summarized in **Table 2**. One of the major drawbacks in the LD is the generation of slopping and spitting, whereas the Q-BOP has neither slopping nor spitting, thus the heat balance and the mass balance in the Q-BOP are more accurately calculated. Reproducibility of uniform metallurgical reactions in the Q-BOP is also superior to the LD. For example, iron oxide in slag exhibits less scatter even in a low carbon range as shown in **Fig. 7**; therefore iron oxide in slag is accurately predicted by being related to the basicity of slag and the carbon content of molten steel.

The above-mentioned aspect of the Q-BOP provides a stabilized decarburization of molten steel, which is

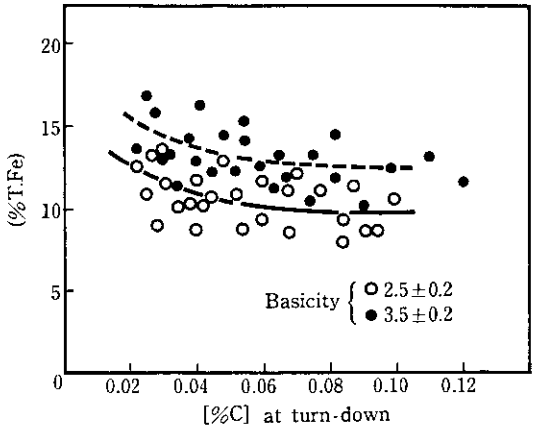

Fig. 7 Relationships of (%T.Fe) in slag and C at end-point

quite favorable for end-point control.

Another important factor is whether or not the data measured by the sensor lance represent a true state of bath. The Q-BOP has neither fire spots on the surface of molten steel nor slag layer at the measuring point; this aspect of the Q-BOP, together with the bath uniformity brought by the intensive gas stirring, is preferable to ensure the reliability of measurement. In fact, carbon contents of samples taken from three different locations in depth show little difference, and the same is also true of the temperature distribution in the bath. A detailed description on this is found elsewhere[4].

Fig. 8 shows the relationship between the predicted carbon content by SMART and the observed one at the end of blow, and **Fig. 9** shows the relationship between the predicted and the observed temperatures; consequently, SMART enables us to predict carbon content and temperature at the end of blow with high accuracy.

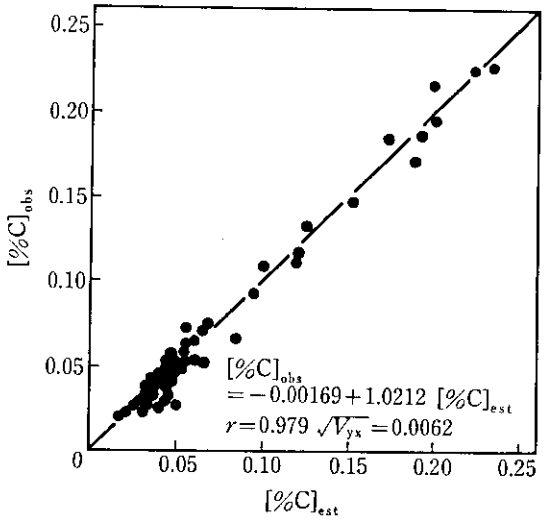

Fig. 8 Comparison of observed carbon content with predicted by SMART

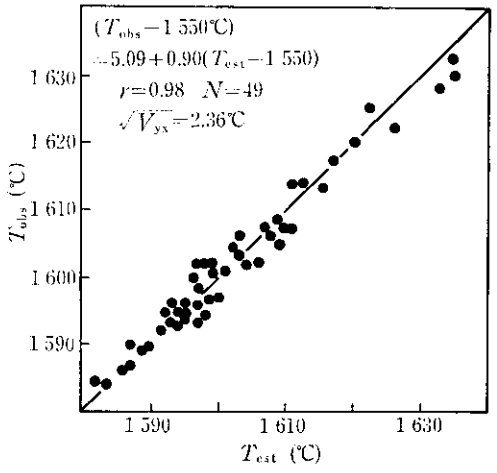

Fig. 9 Comparison of observed temperature with predicted by SMART

After the online operation of SMART, hit rate has rapidly improved, with the highest record of 98.8% attained in July 1979. At the same time, reblow rate has decreased down to the value of 0.8% as shown in **Fig. 10**.

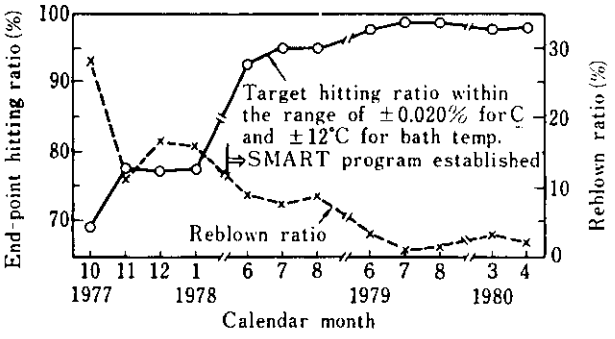

Fig. 10 Monthly variations of hit rate and reblow rate

3.3.2 Quick and direct tapping, "QDT"

Since SMART was completed to control carbon content and temperature at the end of blow, the next step was to establish a reliable technique for the prediction of other components, i.e., manganese, phosphorus and sulfur at the end of blow. For this purpose, statistic analyses were made on the data collected from the begining of Kawasaki's Q-BOP, and finally new technique, QDT has been brought into practical use. The block diagram of QDT is shown in **Fig. 11** which clearly illustrates one of the quick tapping methods. At the final stage of blowing the measurement is carried out by the sensor lance, and if the carbon content and temperature fall in an allowable region which enables to hit the target by some minor corrections for the consumption of oxygen and iron ore, QDT is set up to work; namely tapping is started without measuring temperature or chemical analyses.

As a typical example, predicted manganese contents are compared with observed values in **Fig. 12**, where argreements are sasisfactory. In the same way, phosphorus and sulfur contents at the end of blow are statistically predictable with a high accuracy.

QDT operation has steadily increased in number since start of the online operation as shown in **Fig. 13**, and the time from end-of-blow to tapping rapidly decreased with an increase of QDT operation.

Table 3 shows the advantages of QDT operation brought by both reduction in time from end-of-blow to tapping and decrease in tilting frequency of the furnace. QDT operation reduces temperature drop during tapping by 10 °C. This in turn enables to

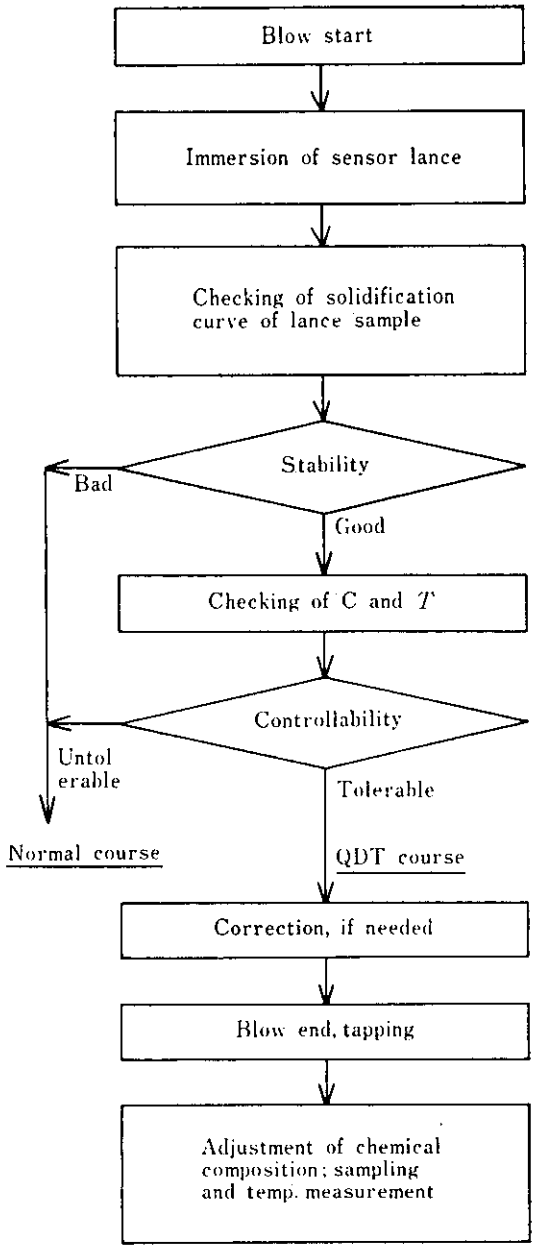

Fig. 11 Block diagram of QDT

decrease tapping temperature by 10 °C, hence the higher iron yield is realized with an increase of the addition of iron ore. Metallic iron in the slag decreases because of the reduction of metal shots in the slag. The total improvement of the bottom life is another important advantage brought by QDT operation as already mentioned above. QDT operation decreases the wearing rate of bottom brick by 0.2 mm per heat in comparison with normal operation as shown in **Fig. 4** and **Table 3**.

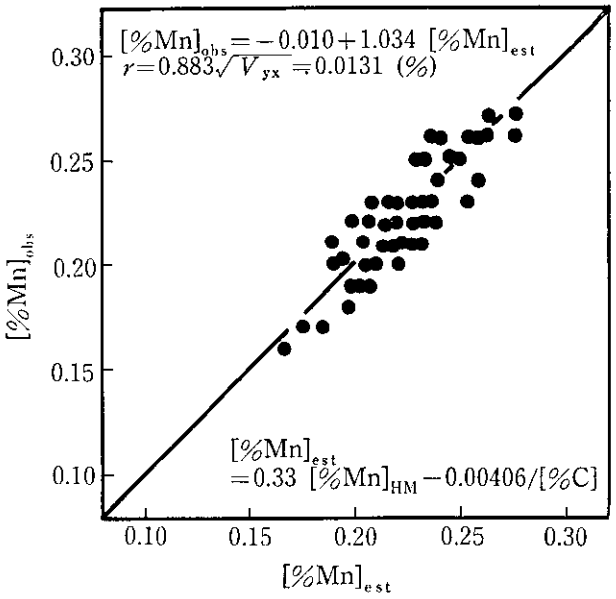

Fig. 12 Comparison of observed Mn with predicted at end of blow

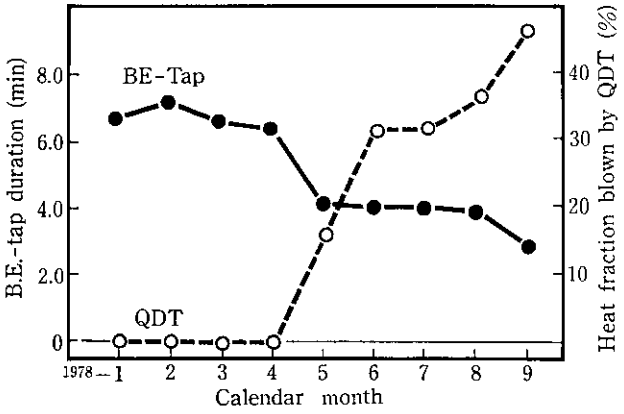

Fig. 13 Monthly variations of QDT ratio and blow-end to tap time

Table 3 Advantages brought by QDT operation

	Remark	
Iron yield	Decrease of temp. drop during tapping Decrease of metallic iron in slag	+0.24%
Refractory conservation	Shortening of blow-end–tap duration Decrease of T.D. index	−0.24 mm/ch
Gas conservation	Decrease of T.D. index	−1.77 nm^3/t
Fe-Mn consumption	Improvement of manganese yield	−0.14 kg/t
High Precision in ladle temp. control	Shortening of blow-end–tap duration	

4 Metallurgical Aspects of Q-BOP[1-2]

On the basis of Kawasaki's data, let us thermodynamically discuss metallurgical reactions taking place in the Q-BOP. **Fig. 14** shows changes of metal composition in the course of blowing. These heats were blown with 100% of hot metal and with oxygen at the rate of 600 to 700 Nm^3/min. Iron ore and mill scales were used as coolants. Samples were taken either by using the sensor lance or by tilting the furnace with intermittent blowing.

Solid oxygen which comes from ore and mill scales is also added to the amount of oxygen shown on abscissa of **Fig. 14**. In comparison with the LD, oxygen efficiency for decarburization in the Q-BOP shows a higher value of nearly 100% at its highest level which, furthermore, lasts quite longer than in the LD as shown by a straight line in **Fig. 14**; consequently, this enables us to save the oxygen consumption per ton of hot metal. As to the LD, some part of solid oxygen is directly transfered into the slag without reduction; thus the oxygen efficiency for decarburization in the LD is not higher than that of the Q-BOP.

Since the total iron content in the slag, as shown in **Fig. 15**, is lower in the Q-BOP than that in the LD, the iron yield is beneficially higher in the Q-BOP. As shown in **Fig. 16**, the oxygen content at the carbon content below 0.10% is lower in the Q-BOP than that of the LD. **Fig. 17** shows the higher yield of manganese at the blowing end of the Q-BOP than that of the LD. These facts ensure a remarkable saving of alloying and deoxidizing elements. As shown in **Fig. 18,** the phosphorus partition of slag to metal is quite higher in the Q-BOP than that of the LD. Although the total iron content is lower in the Q-BOP than in the LD, this causes no handicap in the phosphorus partition as seen in **Fig. 18**; hence we can safely assume that the dephosphorization is enhanced by the injected powdered burnt lime which directly reacts with phosphorus in the bath.

As shown in **Fig. 19**, the amount of burnt lime needed to obtain the same phosphorus content at the end of blow steadily increases with an increase of

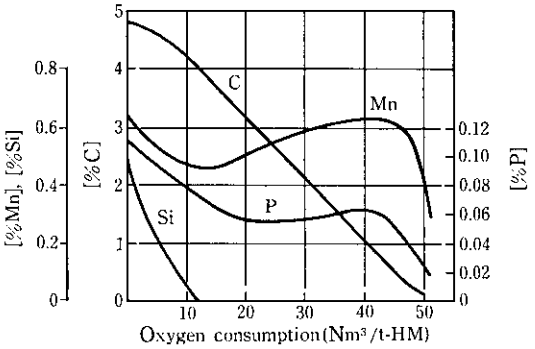

Fig. 14 Changes of bath composition in the course of blowing

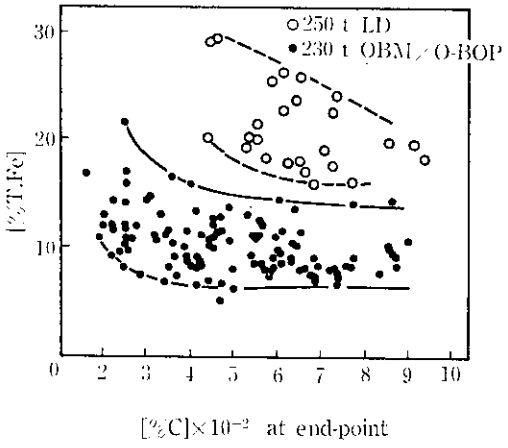

Fig. 15 Relationship of end-point carbon and (%T.Fe) in Slag

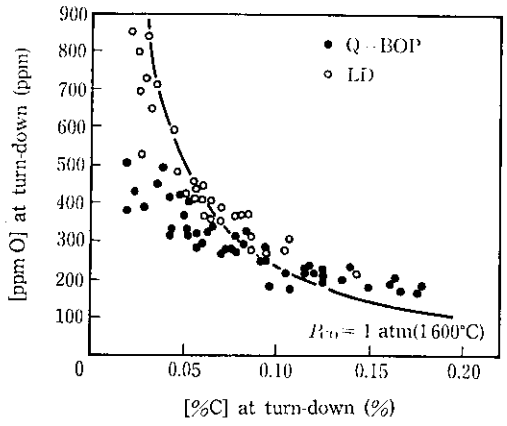

Fig. 16 Carbon vs. oxygen content relationships at turn-down

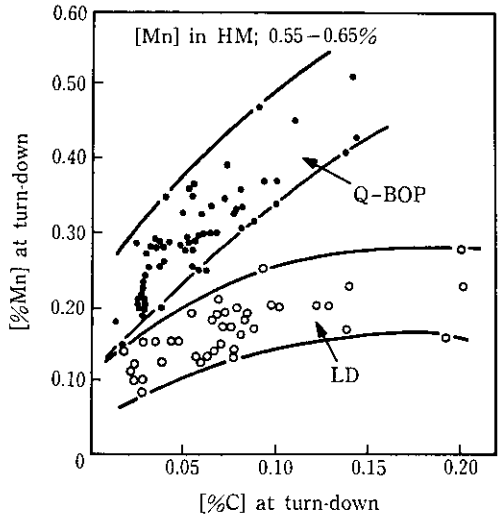

Fig. 17 Manganese vs. carbon content relationships at turn-down

phosphorus content in hot metal. The slope, however, is not so steep as being the case with the LD which is not reproduced here. Therefore the Q-BOP process provides us with an economical method for refining of high phosphorus hot metal.

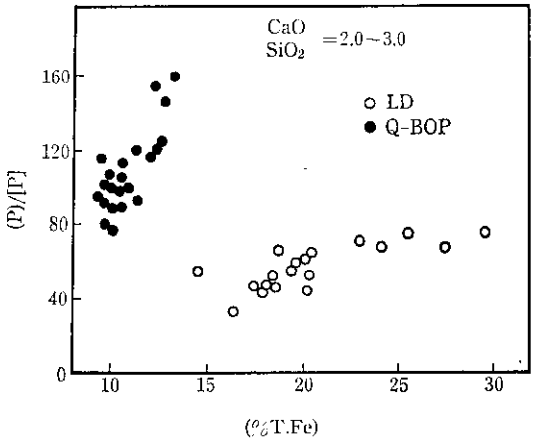

Fig. 18 Influence of (%T.Fe) in slag on phosphorus partition coefficient, (P)/[P]

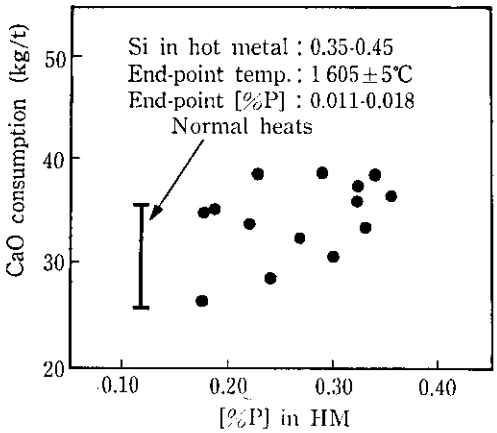

Fig. 19 Influence of phosphorus content in hot metal on consumption of burnt lime

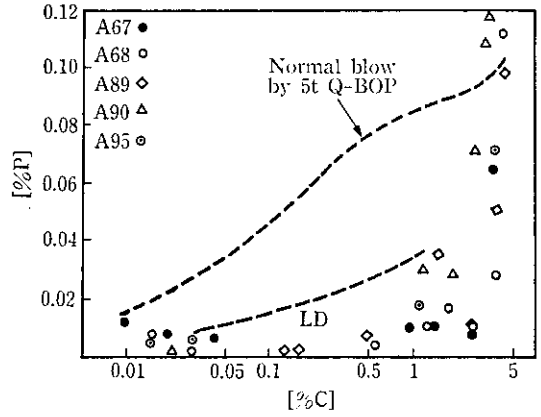

Fig. 20 Enhanced dephosphorization at high carbon level by injection of recycled slags from LD and EF

Fig. 20 shows an enhanced dephosphorization taking place at a high carbon level by injecting recycled slags from the LD or the EF. This is another evidence to support the direct reaction of injected powders with the metal.

The higher sulfur partition is another conspicuous feature of the Q-BOP brought by the lime injection as clearly seen in **Fig. 21**. Nitrogen content at the end of blowing is lower, as shown in **Fig. 22**, in the Q-BOP than in the LD, probably due to the less entrainment of the air from the converter mouth and also due to the steady denitrogenation by the bottom injected oxygen gas.

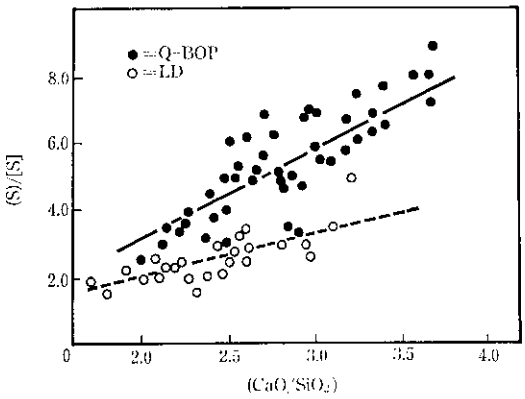

Fig. 21 Effect of basicity on sulfur partition

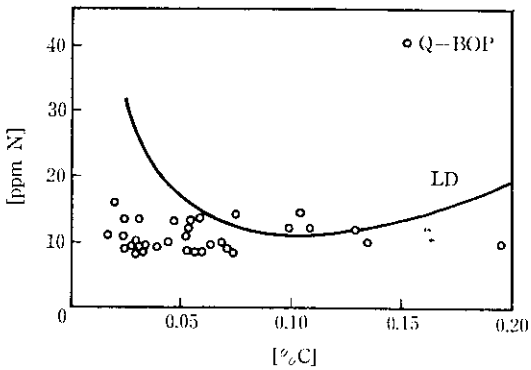

Fig. 22 Carbon vs. nitrogen content relationship at turn-down

5 Physico-Chemical Aspects of Reactions in Q-BOP

As described above, for a given temperature and slag composition, the steel made in the Q-BOP contains more manganese, less oxygen and less sulfur than the steel made in the LD. Also, for a given concentration of carbon in the steel, the total iron content of the slag is less in the Q-BOP than in the LD. These

characteristics can be interpreted in terms of the difference of stirring intensity which significantly affects the state of reactions between slag, steel and gas.

5.1 Decarburization[5]

In comparison with the LD, a strong agitation of the bath in the Q-BOP probably lowers the critical carbon content above which the decarburization rate is controlled by the feeding rate of oxygen. In addition, even at the carbon content below the critical one, the diffusion of carbon in the metal is enhanced by stirring; therefore, the lowest attainable level of carbon in the Q-BOP will be lower than that in the LD.

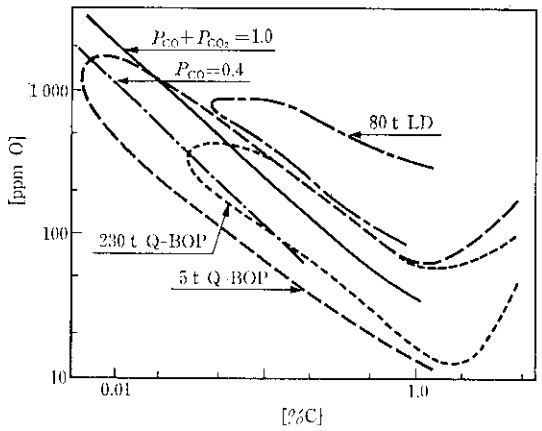

Fig. 23 Carbon vs. oxygen content relationships in Q-BOP and LD

Fig. 23 shows the observed C vs. O relationships compared with the thermodynamical equilibrium ones. Let us assume that the activity of iron oxide in the slag is unity and that the propane injected decomposes into CO, CO_2, H_2, and H_2O, the sum of which is one atmospheric pressure. Then, on the basis of thermodynamics, the carbon content of 0.004% is predicted for the lowest attainable. In fact, we attained the carbon content of 0.006% in the laboratory scale 5 t Q-BOP where economical consideration in terms of iron yield was put aside for experimental purposes. As for the practical 230 t Q-BOP, the carbon content of 0.01% quite lower than 0.02 to 0.025% attainable in the LD was obtained.

As seen in **Fig. 23**, the observed data for the 5 t Q-BOP fall in the range where P_{CO} is close to 0.4 atm, while those for the 230 t Q-BOP fall in the range where the sum of P_{CO} and P_{CO_2} is close to 1 atm. The difference probably comes from the difference of the amount of protective gas relative to oxygen. This difference suggests that the partial pressure of CO in the Q-BOP is easily controlled within a wide range by changing relative flow rates of cooling gas and

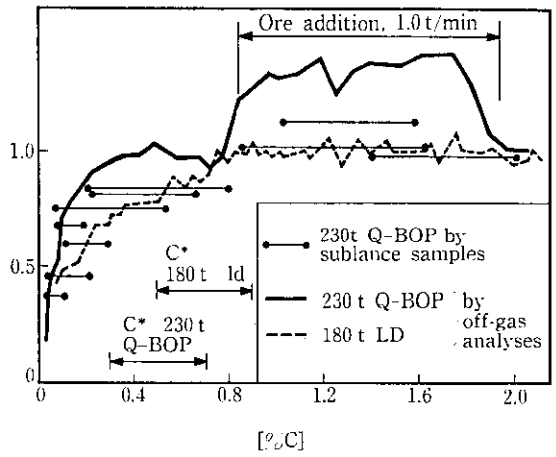

Fig. 24 Relationships of oxygen efficiency for decarburization (η_{O_2}) and carbon content in steel bath

oxygen gas.

Fig. 24 compares the relationships of oxygen efficiency for decarburization and the carbon content in the bath between the Q-BOP and the LD. Here, those curves depicted by solid line and dashed line were obtained by measuring the off-gas composition and its mass flow rate, while the discontinuous horizontal lines were obtained by the carbon contents of the Q-BOP bath measured by the sensor lance. From **Fig. 24** the above-mentioned critical carbon content, C*, is determined to be 0.3 to 0.6% for the 230 t Q-BOP and 0.5 to 1.0% for the 180 t LD, respectively.

Fruehan[6] predicted the value of the gas-metal interfacial area in the Q-BOP based on the rate analysis of denitrogenation. The same analysis yielded the interfacial area (A) of 1.2×10^7 cm² for the 230 t Q-BOP with the oxygen flow rate of 600 Nm³/min. The mass transfer coefficient of carbon (k_C) can safely be assumed, in such an agitated bath as Q-BOP, to be equal to that of nitrogen which is given as 0.03 cm/s. By using A and k_C obtained above, the rate of decarburization controlled by the mass transfer is given by,

$$\frac{dC}{dt} = -0.66C \quad \cdots\cdots\cdots\cdots\cdots\cdots (2)$$

where t is time (min) and C is the carbon content of the bath (%).

On the other hand, when the decarburization rate is controlled by the feeding rate of oxygen, the rate equation is readily obtained by,

$$\frac{dC}{dt} = \frac{-q_0 \times 24 \times 100}{22.4 \times W} \quad \cdots\cdots\cdots (2')$$

where q_0 is the oxygen flow rate (Nm³/min) and W is the weight of the molten steel (kg). By equalizing eqs.

(2) and (2'), the critical carbon content, C*, is evaluated as 0.42% for the Q-BOP which is quite close to the observed value mentioned above; thus the value of A turns out to be reliable enough to predict the size of bubbles dispersed in the bath of the Q-BOP as briefly described below.

Let us put the mean radius of gas bubbles by r (cm) and the total number of gas bubbles in the bath by N. Then A is expressed by

$$A = N \cdot 4\pi r^2 \quad \cdots\cdots (3)$$

Thus, the total gas volume, V (m^3) is given by

$$V = Ar \times 10^{-6}/3 = 4.0r \quad \cdots\cdots (4)$$

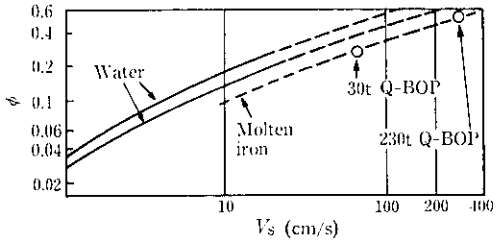

Fig. 25 Empirical relationship of gas hold-up (ϕ) and superficial gas velocity (V_s)

Sano and coworkers[7] experimentally obtained the relationship of the superficial gas velocity (V_s) and the gas hold-up (ϕ) as shown in **Fig. 25**. Here the gas hold-up means the fraction of gas volume in the bath while the superficial gas velocity is the flow rate of gas devided by the horizontal cross-sectional area in the furnace.

ϕ is expressed as,

$$\phi = \frac{V}{V_m + V} \quad \cdots\cdots (5)$$

where V_m is the bath volume (m^3).

At the present case, V_s is calculated to be 3.1 m/s; thus the value ϕ is predicted about 0.5 from **Fig. 25**. Insertion of 0.5 into eq. (5) yields,

$$V = 31.9\ m^3 \quad \cdots\cdots (6)$$

Thus, from eq. (4), r is estimated to be 8 cm. The residence time (t) of a gas bubble is calculated as,

$$t = \frac{31.9\ m^3 \times 60\ s/min}{q_0\ Nm^3/min \times 2 \times (1\,800\ K/300\ K)} \times \frac{1}{1\ atm/1.5\ atm} = 0.34\ s \quad \cdots\cdots (7)$$

These predicted values are helpful to elucidate the physical image of the Q-BOP bath in a visual scope.

At the carbon content less than C*, the rate controlling step for decarburization is the mass transfer of carbon in the melt; hence the decarburization rate is proportional to the carbon content in the bath. In this case the oxygen efficiency for decarburization (η) is given by,

$$\eta = \frac{C - C_e}{C^* - C_e} \quad \cdots\cdots (8)$$

where C_e is the equilibrium carbon content.

Now let us calculate the value of η for the LD at the lowest attainable carbon content of 0.025%. As described above, the critical carbon content C* is given as 0.75%. Undetermined parameter is the equilibrium carbon content C_e for the LD. By assuming the activity of iron oxide in the slag to be unity and the partial pressure of CO is 1 atm, C_e is thermodynamically calculated to be 0.01 to 0.015%. Thus the value of η for the LD is,

$$\eta = \frac{0.025 - 0.012\,5}{0.75 - 0.012\,5} = 0.016\,9 \quad \cdots\cdots (9)$$

Assuming the same value of η, let us calculate the carbon content in the Q-BOP from eq. (8). Substituting η with 0.0169, C_e with 0.004% and C* with 0.42% yields,

$$C = 0.01\% \quad \cdots\cdots (10)$$

The predicted value agrees well with the observed one of 0.01% for the 230 t Q-BOP.

In conclusion, the lowest attainable carbon content is reasonably interpreted in terms of both the critical carbon content C* and the equilibrium carbon content C_e; here C* is the parameter strongly affected by the stirring intensity while C_e^* is the parameter varied by the partial pressure of CO in the furnace.

5.2 Manganese Distribution

If manganese content in the steel is in equilibrium with manganese oxide in the slag, the following equations are valid,

$$(FeO) + \underline{Mn} = (MnO) + Fe \quad \cdots\cdots (11)$$

$$\log \frac{(MnO)}{\underline{Mn}\,(FeO)_t} = \frac{6\,440}{T} - 2.95 \quad \cdots\cdots (12)$$

and

$$(FeO)_t = (FeO) + 1.35\,(Fe_2O_3) \quad \cdots\cdots (13)$$

where T is the absolute temperature (K), (MnO) and $(FeO)_t$ are designated by molar fractions.

As shown in **Fig. 26**, the calculated manganese contents from eqs. (11)–(13) are in good agreement

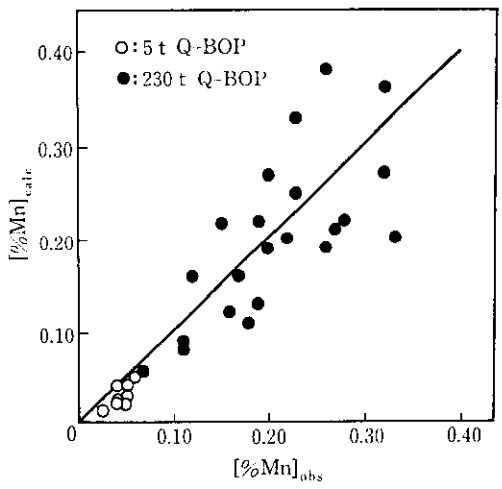

Fig. 26 Comparison of observed manganese content with calculated on an assumption of slag/metal equilibrium

with the observed ones; consequently manganese in the steel is fully in equilibrium with that in the slag.

5.3 Phosphorus Distribution[8]

To calculate the phosphorus partition between slag and metal, the following Healy equation is commonly used and generally valid for the LD.

$$\log\frac{(\mathrm{P})}{[\mathrm{P}]} = \frac{22\,350}{T} + 0.08(\%\mathrm{CaO}) + 2.5\log(\%\mathrm{T.Fe}) - 16.0 \quad \cdots(14)$$

The same calculation was made for the Q-BOP, and the resultant phosphorus partitions were compared with the observed ones. The agreement, however, was not satisfactory. In the Q-BOP, as we have seen above, the iron oxide content in the slag is lower than that

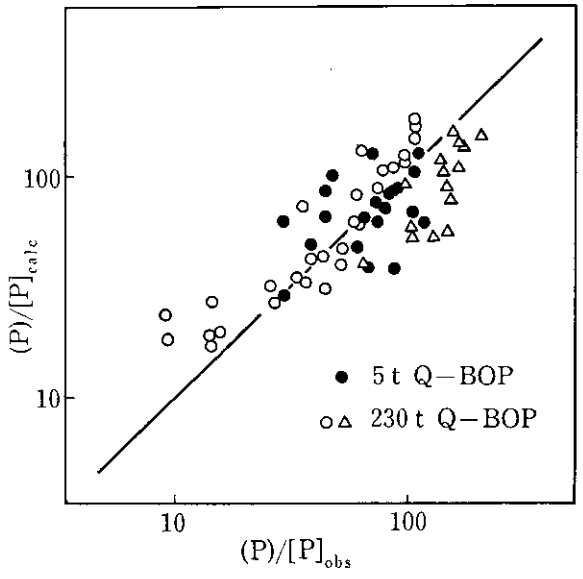

Fig. 27 Comparison of phosphorus partition between observed and statistically calculated

of the LD; hence the oxidizing power of the slag depends not only on the iron oxide but also on the manganese oxide. By using the data of the 5 t Q-BOP and the 230 t Q-BOP, the following empirical equation was statistically derived for the phosphorus partition in the Q-BOP.

$$\log\frac{(\mathrm{P})}{[\mathrm{P}]} = \frac{10\,773}{T} + 0.655\log(\%\mathrm{T.Fe}) + 3.273\log(\%\mathrm{CaO}) + 1.133\log(\%\mathrm{MnO}) - 0.822\log[\%\mathrm{Mn}] - 11.362 \quad \cdots(15)$$

As shown in **Fig. 27,** the calculated partitions are in a better agreement with the observed ones than those computed by the Healy equation.

5.4 Stirring Intensity and Metallurgical Reactions[9, 10]

Since we have been quite familiar with the process of the LD, it seems worthwhile to clarify what is a governing factor which distingushes the Q-BOP from the LD. With this view in mind, let us find out an optimum parameter in terms of which we can comprehensively interpret all the oxidizing refining furnaces such as the Q-BOP, the LD, and the AOD.

Decarburization and oxidation of iron are two of the main metallurgical reactions taking place in oxidizing steelmaking furnaces and are often put in contrast with each other. If the former reaction takes precedence over the latter, a lower concentration of carbon will be attained without significant loss of easily oxidizable elements such as Cr in the bath; hence, the furnace is regarded preferable for the production of stainless steels.

On the other hand, if the oxidation of iron takes precedence over the decarburization, the high oxygen potential is realized in the slag and the reaction of dephosphorization proceeds quite easily; the so-called soft blowing practice in the LD is referred to as the refining of this type. When we construct a suitable parameter, we should give this matter greater consideration.

In the first place, the selective oxidation of carbon in the bath is determined by the value of the partial pressure of CO gas in the furnace, namely the smaller the partial pressure, the lower the attainable content of carbon in the bath. Secondly, the parameter must contain a term of interaction of oxygen and iron. So far, the characteristic of oxidizing refining furnaces was discussed solely in terms of the flow rate of oxygen per unit weight of the bath. Although this is of prime interest, so long as we discuss the productivity of a furnace, it fails in explaining not only the difference of the LD and the Q-BOP, but also that of the soft

blowing and the hard blowing practices in the LD.

Even if the same amount of oxygen is supplied per unit time, the bulk of the steel in the Q-BOP has much more chance to come into contact with the oxygen than that in the LD does because of the difference of their mixing intensities. With regard to a term composing the parameter, we select the ratio of the flow rate of oxygen to that of the bath which is given by the weight of the bath divided by the time required for perfect mixing of a tracer. A small value of the ratio means that the oxidation of carbon has priority.

Let us define a parameter, ISCO (Index for Selective Carbon Oxidation) by the following equation:

$$\mathrm{ISCO} = \left(\frac{2Q_{O_2}}{2Q_{O_2} + Q_d}\right)\left(\frac{Q_{O_2}}{W/\tau}\right) \quad \cdots\cdots (16)$$

where Q_{O_2} is the oxygen flow rate (Nm³/min), Q_d is the flow rate of argon, nitrogen or decomposed coolant-gas effective to dilute the partial pressure of CO gas (Nm³/min), W is the weight of molten iron (t) and τ is the mixing time of the bath (s).

On the right hand side of eq **(16)**, the term in the first parentheses is the partial pressure of CO gas and regarded a chemical term while the term in the second is the ratio of the flow rate of oxygen to that of steel and is regarded a kinetic term; the smaller the magnitude of the product of the first and the second terms, the oxidation of carbon is ensured down to a lower concentration without appreciable oxidation of other components such as iron or chromium. Change of phosphorus content during blowing in the Q-BOP and the LD with decreasing carbon content at [%C] $\eqslantless$ 1 has found unified interpretation in terms of ISCO. This is shown in **Fig. 28**. As ISCO becomes smaller, carbon is preferentially oxidized to iron, resulting in retarded dephosphorization and hence higher phosphorus content at [%C] $\geqq$ 1. Consequently, the ratio of dephosphorization rate to decarburization rate becomes larger, reflecting the higher phosphorus content for smaller ISCO value at [%C] $\leqq$ 1.

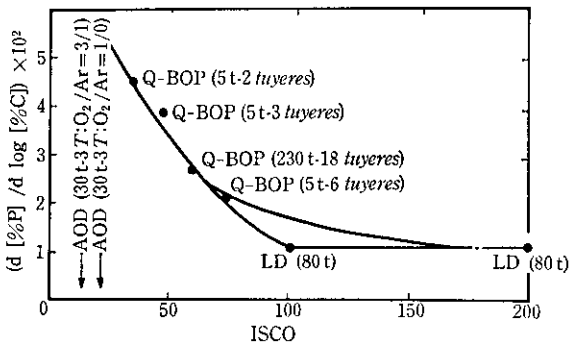

Fig. 28 Ratio of dephosphorization rate to decarburization rate as a function of ISCO

To demonstrate another example for the validity of ISCO, the blowing of high chromium bath was conducted by using the 5 t Q-BOP. The blowing procedures are briefly described below. Firstly the hot metal (5 t) was blown and decarburization and dephosphorization were completed. After the slag was decanted, Fe-Cr alloy (1.8 t, 7%C, 7%Si, and 65%Cr) was added into the bath and the second blowing was subsequently carried out by using the mixture of oxygen and nitrogen. In the course of the second blowing, intermediate samples were taken for chemical analyses.

Fig. 29 shows the amounts of chromium oxidized depending on the carbon contents in the bath. In these figures, the data of the AOD are also shown referring to the literature[13].

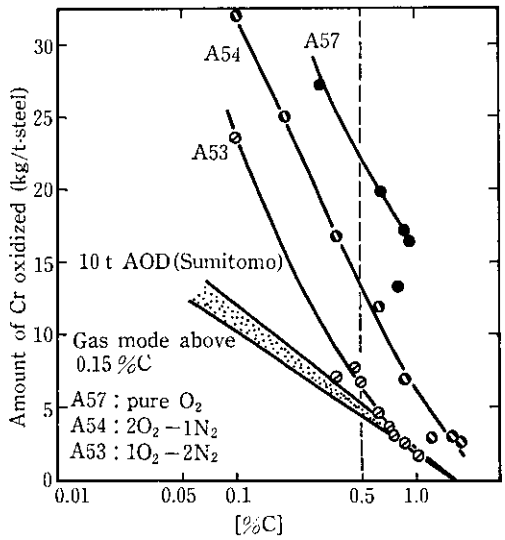

Fig. 29 Amount of chromium oxidized during blowing with different ISCO's

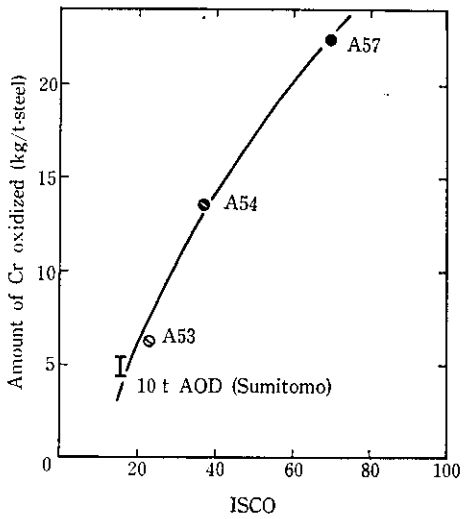

Fig. 30 Interpretation of chromium oxidation in terms of ISCO

During the second blowing down to the carbon content of 0.5%, the value of ISCO was kept constant in each heat. Hence, the amounts of chromium oxidized were measured at the carbon content of 0.5% and they are compared with the values of ISCO as shown in **Fig. 30**, where a surprisingly good correlation is found between ISCO and chromium-loss in the bath. Consequently, **Fig. 30** provides us with an alternative demonstration on the validity of the parameter, ISCO, which characterizes metallurgical reactions in oxidizing refining furnaces.

6 Concluding Remarks

Recent developments of the OMB/Q-BOP steelmaking have been described. By using proper refractories together with the improved brickwork and the slag coating technique, Kawasaki has succeeded in prolongation of the bottom life of the Q-BOP: 2 063 heats at the maximum and 1 500 heats on an average. For the purpose of choosing the best refractory out of many types of commercial ones, a new testing method, "Panel AE Spalling Test" has successfully been developed. By using this, the magnesia-carbon brick has been found to be the most preferable for the bottom refractories of the Q-BOP.

The OG gas of the Q-BOP contains much more CO and H_2 components than those of the LD; hence the latent heat exceeds 2 700 kcal/Nm³. About 86.4% of the total off-gas energy is recovered as OG gas and steam.

As to the end-point control, the Q-BOP is superior to the LD because of the compositional uniformity and reproducibility in the bath. Kawasaki has completed the dynamic control system "SMART" which stands for System for Measuring and Attaining Refining Target. SMART, upon its successful completion as online function, has contributed to a marked improvement of hit rate for both carbon and temperature at turn-down with the highest record of 98.8%.

On the basis of a reliable method for the prediction of manganese, phosphorus and sulfur contents at the end of blow, SMART has further been developed into a new technology called QDT (Quick and Direct Tapping), which brings much benefit.

For a given temperature and slag composition, the steel made in the Q-BOP contains more manganese, less oxygen and less sulfur than the steel made in the LD. In addition, for a given carbon content in the steel, the total iron content of the slag is less in the Q-BOP than in the LD. These favorable aspects enable us to obtain a higher yield of iron, and to save alloying and deoxidizing agents.

The above-mentioned metallurgical characteristics are attributable to an intensive stirring of the bath in the Q-BOP in comparison with the LD; therefore the states of the metal, the slag and the gas are close to the thermodynamic equilibrium. The lowest possible carbon level in the Q-BOP is 0.01% while blowing oxygen, and 0.006% by rinsing with inert gas. Both are quite lower than those of the LD.

To comprehensively interpret all the oxidizing refining furnaces such as the Q-BOP, the LD and the AOD, a new parameter ISCO (Index for Selective Carbon Oxidation) has been proposed. ISCO consists of a chemical term corresponding to the partial pressure of CO and a kinetic term corresponding to the relative mass flow rate of oxygen and molten steel. The values of ISCO are evaluated for the LD, the Q-BOP and the AOD; they become smaller in this order. The validity of ISCO has been verified for the following two cases; one is for the relation of decarburization rate and dephosphorization rate, and the other is for the relation of decarburization rate and chromium oxidation at the refining of stainless steel.

References

1) T. Ohta: Kogyo to Seihin, (1979) 61, pp. 127–133.
2) M. Saigusa, J. Nagai, F. Sudo, H. Bada and S. Yamada: Proceedings of Developments in Metallurgical Control in Basic Oxygen Steelmaking, S. G. Thomas Centenary Celebrations, BSC, Redcar, (1979), Paper 9.
3) R. Uchimura: Kawasaki Steel Technical Report, **11** (1979) 1, pp. 132–142.
4) S. Yamada, H. Bada, F. Sudo, J. Nagai, M. Saigusa and K. Nakanishi: presented at the Annual Meeting of AIME held in Washington DC., March (1980).
5) K. Nakanishi, K. Suzuki, N. Bessho, N. Nakamura and H. Bada: Tetsu-to-Hagane, **64** (1978), S 168.
6) R. J. Fruehan: Ironmaking and Steelmaking, (1976) 1, p. 33.
7) M. Sano and K. Mori: Tetsu-to-Hagane, **63** (1977), S 576.
8) T. Nozaki, N. Harada, H. Nakamura, K. Nakanishi, F. Sudo and S. Yamada: Tetsu-to-Hagane, **65** (1979), S 199.
9) K. Nakanishi, Y. Kato, K. Suzuki and J. Katsuki: Tetsu-to-Hagane, **64** (1978), S 169.
10) K. Nakanishi, T. Nozaki, Y. Kato and J. Katsuki: 7th Japan-USSR Joint Symposium on Physical Cemistry of Steelmaking, Moscow, May (1979).
11) K. Nakanishi, T. Fujii and J. Szekely: Ironmaking and Steelmaking (Quarterly), (1975) 3, p. 193.
12) A. Chatterjee, N. O. Lindfors and J. A. Wester: Ironmaking and Steelmaking (1976) 1, p. 21.
13) K. Ishikawa, T. Sakane, M. Hattori and H. Kodama: Tetsu-to-Hagane, **64** (1978) 4, S 182.
14) T. Ohta, M. Saigusa, J. Nagai, F. Sudo, K. Nakanishi, T. Nozaki and R. Uchimura: Kawasaki Steel Technical Report, **12** (1980) 2, p. 1.